Surface Wave Tomography Applied to the North American Upper Mantle

Suzan van der Lee

Department of Geological Sciences, Northwestern University, Evanston, Illinois, USA.

Andrew Frederiksen

Department of Geological Sciences, University of Manitoba, Winnipeg, Manitoba, Canada.

Tomographic techniques that invert seismic surface waves for 3-D Earth structure differ in their definitions of data and the forward problem as well as in the parameterization of the tomographic model. However, all such techniques have in common that the tomographic inverse problem involves solving a large and mixed-determined set of linear equations. Consequently these inverse problems have multiple solutions and inherently undefinable accuracy. Smoother and rougher tomographic models are found with rougher (confined to great circle path) and smoother (finite-width) sensitivity kernels, respectively. A powerful, well-tested method of surface wave tomography (Partitioned Waveform Inversion) is based on inverting the waveforms of wave trains comprising regional *S* and surface waves from at least hundreds of seismograms for 3-D variations in *S* wave velocity. We apply this method to nearly 1400 seismograms recorded by digital broadband seismic stations in North America. The new 3-D *S*-velocity model, NA04, is consistent with previous findings that are based on separate, overlapping data sets. The merging of US and Canadian data sets, adding Canadian recordings of Mexican earthquakes, and combining fundamental-mode with higher-mode waveforms provides superior resolution, in particular in the US-Canada border region and the deep upper mantle.

NA04 shows that 1) the Atlantic upper mantle is seismically faster than the Pacific upper mantle, 2) the uppermost mantle beneath Precambrian North America could be one and a half times as rigid as the upper mantle beneath Meso- and Cenozoic North America, with the upper mantle beneath Paleozoic North America being intermediate in seismic rigidity, 3) upper-mantle structure varies laterally within these geologic-age domains, and 4) the distribution of high-velocity anomalies in the deep upper mantle aligns with lower mantle images of the subducted Farallon and Kula plates and indicate that trailing fragments of these subducted oceanic plates still reside in the transition zone. The thickness of the high-velocity layer beneath Precambrian North America is estimated to be 250 $\pm$ 70 km thick. On a smaller scale NA04 shows 1) high-velocities associated with subduction of

Seismic Earth: Array Analysis of Broadband Seismograms
Geophysical Monograph Series 157

10.1029/157GM05

the Pacific plate beneath the Aleutian arc, 2) the absence of expected high velocities in the upper mantle beneath the Wyoming craton, 3) a V-shaped dent below 150 km in the high-velocity cratonic lithosphere beneath New England, 4) the cratonic lithosphere beneath Precambrian North America being confined southwest of Baffin Bay, west of the Appalachians, north of the Ouachitas, east of the Rocky Mountains, and south of the Arctic Ocean, 5) the cratonic lithosphere beneath the Canadian shield having higher *S*-velocities than that beneath Precambrian basement that is covered with Phanerozoic sediments, 6) the lowest *S* velocities are concentrated beneath the Gulf of California, northern Mexico, and the Basin and Range Province.

1. INTRODUCTION

Normal mode frequencies and *P* and *S* travel times have established reference models for seismic velocity of the Earth's mantle since early last century. These models are one-dimensional (1-D) in that the velocity varies only with depth [*Dziewonski et al.*, 1975; *Jeffreys and Bullen*, 1940; *Kennett et al.*, 1995]. Seismic tomography, introduced in the nineteen seventies, utilizes the arrival time residuals not explained by the 1-D reference model (*Aki et al.*, 1977) or surface and mantle wave propagation not explained by the modes computed for the reference model (*Dziewonski et al.*, 1977) to infer the 3-D distribution of seismic velocity. *Seismic tomograpy* is a form of computer-aided tomography (CAT), a computational technique that allows looking into the interior of a body without actually slicing it up. In an analogy to cutting a rock into thin sections, *seismic tomography* computes thin sections of the Earth's interior, by extracting the relevant information from observed seismic waves.

The propagation of seismic surface waves is governed by the material properties, in particular the rigidity, of the crust and mantle through which they pass. The material property best constrained by surface waves is the *S*-wave velocity, which depends on the square root of rigidity. Cold material, e.g. the lithosphere, is relatively rigid, thus speeding up the *S* and surface waves that propagate through it. Weak material, such as the asthenosphere, slows these waves down.

Modern digital broadband seismic stations have the ability to record surface waves, which have large amplitudes between 10 and 100 mHz. With 70 km between broadband stations, the transportable array component of the USArray project will thus provide a wealth of surface wave data, with which we can advance tomographic imaging of the mantle and crust beneath the US and surrounding regions.

In surface wave tomography 3-D *S*-velocity models are constructed from the properties of surface waves recorded at such broadband seismic stations. Tomographic techniques using seismic surface waves differ in their definitions and use of data, parameterization of the tomographic model, and definition of the forward problem. However, all these techniques have in common that the tomographic inverse problem, i.e. extracting elastic properties of the Earth's mantle and crust from surface waves observed in seismograms, is at one point defined as a mixed determined set of linear equations. Consequently these inverse problems have multiple solutions—any one solution is said to be non-unique—and inherently undefinable accuracy. The quality and robustness of tomographic models are assessed most commonly through resolution tests, but also through comparisons of models derived with different data, model parameterizations, or problem definitions.

In this paper, at the advent of USArray, we list a variety of surface wave tomographic techniques. We demonstrate the application of one such technique, Partitioned Waveform Inversion (PWI) [*Nolet*, 1990], to a data set of fundamental and higher mode Rayleigh wave forms from nearly 1400 regional seismograms recorded at North American digital broadband seismic stations (Figure 1).

The USArray data set and theoretical advances discussed elsewhere in this book will dramatically improve the data's resolving power, the tomographic model's uniqueness, and our ability to model the data. Nevertheless, the model derived and presented here can be a useful starting point. It can be used to target areas for the portable component of the USArray project, to reduce non-linearities in future tomographic inversions, or to estimate the mantle contribution to observed gravity, just to name a few.

2. OVERVIEW OF THE STUDY REGION

The North American tectonic plate is bound by spreading mid-oceanic ridges to its north and east and by transform faults and subduction zones to its south and west. The latter are hosted by or adjacent to the North American continent,

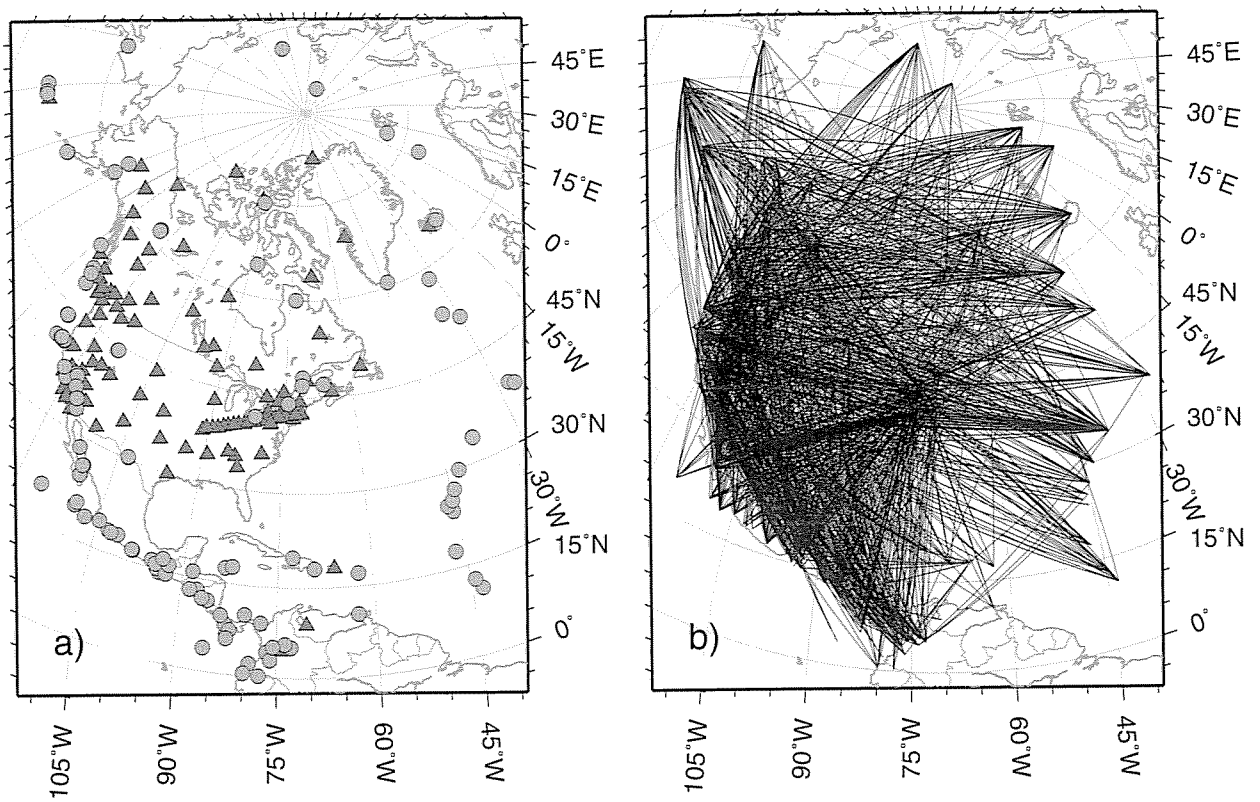

Figure 1. a) Epicenters of used earthquakes (bullets) and used seismic stations (triangles). b) Corresponding great-circle wave path coverage. The merged and expanded data set used is described in the text.

while the former are beneath the Atlantic and Arctic oceans relatively far from the continent. Tectonic activity is associated with the current positions of these plate boundaries, but is also spread out in Cenozoic and Mesozoic tectonic domains, such as the Basin and Range Province. The most spectacular topographic feature is the Rocky Mountain Belt, which formed in the Meso- and Cenozoic as a result of the northeast-dipping subduction of the enormous, oceanic Farallon and Kula plates beneath North America [*Engebretson et al.*, 1985; *Stock and Molnar*, 1988]. The Rocky Mountains mark the boundary between tectonically active and tectonically stable North America. A large part of tectonically stable North America is covered with Phanerozoic sediments but is a Precambrian tectonic domain as it has not been tectonically active since the Grenville at 1 Ga [*Hoffman*, 1988]. The Archean and Proterozoic geology of stable North America is exposed in the Canadan shield, comprising most of Canada. The eastern North American margin and Appalachian Mountain Belt have a tectonic origin in the Paleozoic. The Appalachian and Rocky mountain belts straddle Precambrian North America. North America spans the largest range of geologic ages, with the oldest rocks (4 Ga) in the Slave Province of the Canadian Shield [*Stern and Bleeker*, 1998; *Bowring and Williams*, 1999] and the youngest (0 Ma) at various volcanically active locations, such as Yellowstone, the Cascades, Aleutians, and Trans Mexican Volcanic Belt.

Seismic tomography on various scales with various data and methods has unambiguously shown that the North American tectonic domains of different geologic ages are correlated with distinct uppermost mantle structures; for example, the upper few hundreds of km beneath Precambrian North America are colder and more rigid than the upper mantle beneath tectonically active North America. Global seismic tomography first outlined the contrast in upper-mantle properties across the Rocky Mountain front, but the magnitude and sharpness of the contrast became clear from regional tomographic studies, such as the pioneering study of *Grand* [1994]. This early work by *Grand* [1994] also found evidence for Farallon subduction in the top of the lower mantle and later work [*Van der Lee and Nolet*, 1997a] suggested that the trailing fragments of the subducted Farallon plate still reside in the (deep) upper mantle. Comparing seismic images with reconstructions of past configurations of tectonic plates and surface geologic history will provide important constraints on deep mantle processes. Closer to the

surface, studying the correlations between geology, tectonic history, xenolith analyses, and high-resolution seismic tomography, such as that expected from USArray, will provide us with important clues to the evolution of continents [e.g. *Van der Lee*, 2001].

3. SURFACE WAVE TOMOGRAPHY

3.1. Definition of data

A straightforward way to define data is as the discretely sampled values of the instrument-deconvolved, windowed and filtered surface wave train [*Nolet*, 1990; *Xu and Wiens*, 1997; *Ekström and Dziewonski*, 1998]. Another way, with roots in the era of analogue seismograms, is to derive secondary observables from the recorded seismogram, usually in the form of frequency and time dependent travel time delays or phase and group velocities [*Gee and Jordan*, 1992; *Cara*, 1979; *Wu et al.*, 1997; *Nishimura and Forsyth*, 1989]. Such data can be extracted from observed seismograms through a series of filters, windows and crosscorrelations [*Herrin and Goforth*, 1977; *Gee and Jordan*, 1992].

In Nolet's original PWI method, we apply time windows and frequency filters interactively in order to select coherent waves and to remove incoherent ones. Frequency bands used for the model presented here are within 6 to 80 mHz, where the uppermost limit decreases rapidly with increasing length of the wave path. Over 90 % of the seismograms have upper limits of 30 to 60 mHz. Many have lower limits somewhat over 10 mHz, to eliminate long-period noise. For the same reason and to justify the assumption of independent propagation for each mode we limit the time window to begin after the arrival times of *S* waves that turned in the lower mantle and to end before the arrival of the first scattered fundamental mode energy, usually towards the middle and end of the direct fundamental mode Rayleigh wave train. We often use two consecutive time windows, which can overlap and have different frequency contents, but do not need to strictly separate modes. In some recent applications of PWI, the interactive part was replaced by an automatic waveform selection and fitting procedure [*Lebedev and Nolet*, 2003]. While the automatic version is most efficiently used for large volumes of similar and long-distance seismograms [*Lebedev and Nolet*, 2003], the interactive method is most effectively used in structurally complex regions with a wide variety of seismicity and seismography [*Marone et al.*, 2004].

3.2. Model parameterization

A first generation of global tomographic models was built up from a series of spherical harmonic functions with decreasing wavelength [*Dziewonski*, 1977; *Li and Romanowicz*, 1996; *Woodward and Masters*, 1991]. On a regional scale, *Nishimura and Forsyth* [1989] used a geologically meaningful model parameterization. They used magnetic seafloor anomalies to subdivide their study region in elongated areas of different average geologic age and inverted surface wave group delay times for seismic velocity that was constant in each of these regions. Later global models and regional models were based on a series of cells or blocks of constant seismic velocity, that were equidistant in latitude and longitude but not in depth [*Zielhuis and Nolet*, 1994; *Snieder*, 1988]. A next generation used a Cartesian grid of nodes for 3-D velocity anomalies and a spherical mesh of triangles for spatial variatios in Moho depth [*Van der Lee and Nolet*, 1997b]. Velocity (and Moho depth) is defined through linear or spline interpolation between the nodes [*Van der Lee and Nolet*, 1997b; *Boschi and Ekström*, 2002]. Currently, more and more tomographic models are based on regionally varying model parameterization, where the model has more parameters (blocks, nodes, cells) in regions of dense wave path coverage and fewer in regions of sparse wave path coverage [*Boschi et al.*, 2004; *Pilidou et al.*, 2004]. This adaptive gridding emulates regionally varying regularization constraints in a highly cpu-efficient manner.

In this paper's application of PWI, we parameterized the 3-D Earth in a Cartesian framework [*Nolet*, 1993]. The spacing between the knots of this Cartesian grid is 100 km in the x and y directions and 60 km in the z direction. The grid represents the 3-D *S*-velocity structure of the upper mantle and crust. In the damped linear inversion, we searched for an a priori smooth model. To avoid biasing our model with an interpreted crustal model, we allowed the crustal velocity and the Mohorovicic discontinuity (Moho) depth to vary in the inversion. We further constrain the depth to the Moho by using the database of *Chulick and Mooney* [2002]. Technical details can be found in *Van der Lee and Nolet* [1997b] and *Frederiksen et al.* [2001].

3.3. Definition of the forward problem

The forward problem links the model parameters (seismic velocities) to the data (wave forms, delay times, group or phase velocities). The forward problem involves the computation of synthetic seismograms or at least of phase or group velocities and their partial derivatives to the model parameters. Generally the great circle approximation is used for the sensitivity of the data to the model, which means that only anomalies directly on the great circle path contribute to the predicted data (Figure 2a). In the first part of PWI the average velocity structure along each wave path is determined by optimally fitting the waveforms of each seismogram with

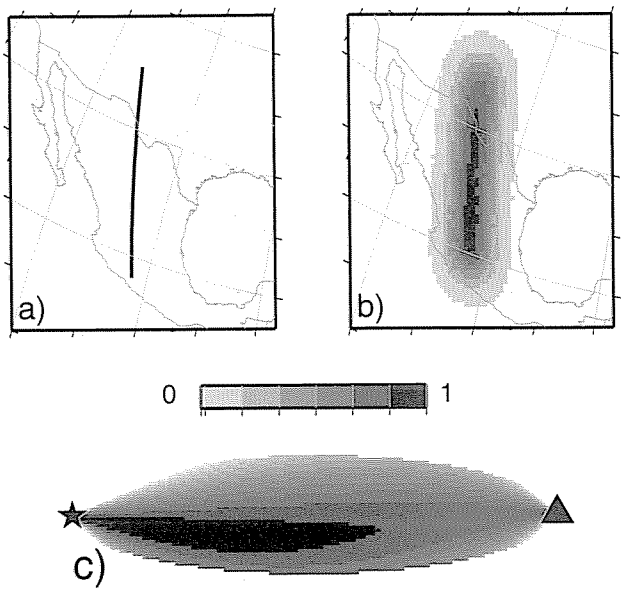

Figure 2. a) Example of a sensitivity kernel in the great-circle approximation. b) Example of a sensitivity kernel that includes an amount of off great circle sensitivity. c) An approximation of a finite-width sensitivity kernel [*Van der Lee*, 1998], which also takes the source radiation pattern into account. Note that sensitivity is greatest near the receiver, asymmetric, and highest near the lobe of the source radiation pattern.

synthetic waveforms. We construct synthetic seismograms by the summation of 20 mode branches, with phase velocities between 1 and 20 km/s. This yields accurate seismograms, for a weakly heterogeneous Earth, in the limited time window from the *S* wave to the Rayleigh wave, for epicentral distances up to at least 70°. Most paths in our data set are about half that distance. We use the Harvard centroid moment tensor solution (Dziewonski et al., 1992) for the computation of mode excitation factors.

In PWI we used multiple background models, each with a different crustal thickness and ocean depth, for the construction of synthetic seismograms. Using different background models for each wave path improves the initial fits substantially and reduces effects possibly introduced by the weakly non-linear dependence of phase velocity on *S* velocity. In addition, we account for local Earth structure beneath the source and station by assuming local Earth models to compute excitation factors and station amplitudes [*Levshin*, 1985; *Tromp and Dahlen*, 1992]. A different way in which these non-linear effects can be reduced is to use local sensitivity kernels, derived for a 3-D rather than a 1-D Earth model [*Boschi and Ekström*, 2002].

An increasingly popular modification of the great circle approximation is to replace the great circle by a sensitivity kernel with a finite width across the great-circle path [*Yoshizawa and Kennett*, 2002; *Ritzwoller et al.*, 2002]. With sensitivity distributed symmetrically across the great circle path this approach represents a step in the direction of using physical sensitivity kernels in surface wave tomography, which take a variety of shapes but generally do neither distribute sensitivity symmetrically across the great circle path, nor concentrate it on the great-circle path (Figure 2c) [*Meier et al.*, 1997; *Marquering et al.*, 1998; *Zhao et al.*, 1998, *Spetzler et al.*, 2002, *Zhou et al.*, 2004]. Replacing great circle paths by smoother, finite-width sensitivity kernels in the forward computation has the effect of shifting the smoothing operation from the model vector to the sensitivity matrix. Plate 2 demonstrates this effect by showing our new model, NA04, derived with great circle path-averaging sensitivity (Figure 2a), along with a model derived with the same regularization parameters but with a smoother, finite-width sensitivity kernel (Figure 2b). The latter sensitivity kernels were computed simply by smoothing the great circle path sensitivity with a standard smoothing operator. Both models (Plate 2), though different, fit the data equally well by definition (see next section). However, the model (Plate 2b) with the smoother sensitivity is less smooth than the model (Plate 2a) with the less smooth (path-averaging) sensitivity.

A more sophisticated approach to the surface-wave sensitivity problem is to incorporate more realistic physics into the forward modeling approach. Sharp 3-D structure will produce mode coupling effects as well as scattered surface waves, neither of which are considered in the path-averaging approach. Including mode coupling [*Marquering and Snieder*, 1995; *Li and Romanowicz*, 1996] results in sensitivity kernels in which the depth sensitivity varies along the great-circle path. An approximation to taking off-path sensitivity into account requires calculation of the Fresnel zone for surface waves [*Yoshizawa and Kennett*, 2002]. *Meier et al.* [1997], *Spetzler et al.* [2002], and *Zhou et al.* [2004] use Born and Rytov single-scattering theory to calculate realistic finite-width sensitivity kernels. *Lebedev and Nolet* [2003] used such kernels in an application of PWI to southeast Asia. A complete approach, incorporating multiple scattering and mode coupling, has been developed and used by *Friederich* [2003] to invert full broadband seismograms, albeit at considerable computational expense.

Physically realistic sensitivity kernels have finite widths and are generally smoother than sensitivity kernels confined to great circle paths. As such they would tend to relatively rough velocity models, as in the simple experiment results shown in Plate 2. However, the benefit of physically realistic sensitivity kernels lies in their expected ability to construct a more consistent system of seismogram-derived equations

than possible with path-averaging theory. The solution of a more consistent system of equations would fit the combined seismograms better than path-averaging theory would under comparable regularization biases.

If scattering theory is not incorporated in surface-wave sensitivity kernels, possible off-path scattered energy will represent an unmodeled component of the seismogram. Excluding scattered energy is usually accomplished through a delicate selection of time windows and frequency bands, which can be a finicky and laborious process. An important advance offered by the USArray component of Earthscope is its configuration in dense arrays. Transmitted and scattered waveforms can then be separated over clusters of stations with array processing techniques; off-path energy will display different move-out behavior over the cluster and could be suppressed by beam-forming. This would enable a two-stage inversion procedure, in which a ray-theoretical approach would be used to determine smooth structure from beam-formed seismograms, and scattering theory would be used to incorporate the residual scattered energy, which can be separated form other "noise" by secondary beam-forming, and sharpen the velocity model.

3.4. *Inverse problem*

At one or more stages of surface wave tomography a discrete, linear, mixed-determined inverse problem needs to be solved. This entails finding a model vector $\boldsymbol{m}$ (containing the model parameters) that combines with the sensitivity matrix $\boldsymbol{G}$ (containing the forward theory) in such a way that the (primary or secondary) data vector $\boldsymbol{q}$ is matched as closely as possible. Generally, a "close" match is defined in a least-squares sense and thus found by minimizing $(\boldsymbol{Gm}-\boldsymbol{q})^{\mathrm{T}}(\boldsymbol{Gm}-\boldsymbol{q})$.

The two solution methods most widely used in surface wave tomography are a regularized least-squares inversion and singular value decomposition (SVD). For mixed-determined inverse problems SVD yields a minimum-norm, least-squares solution. A direct least-squares solution can be obtained through $\boldsymbol{m} = (\boldsymbol{G}^{\mathrm{T}}\boldsymbol{G}+\varepsilon^2\boldsymbol{R}^{\mathrm{T}}\boldsymbol{R})^{-1}\boldsymbol{q}$, where $\boldsymbol{R}$ is a regularization matrix, taking the form of the identity matrix $\boldsymbol{I}$ in a least-squares inversion that is regularized through damping. Such an evaluation, however, has traditionally been prohibitive because of the enormous size of tomographic inverse problems and limited computational power. The direct evaluation has been replaced by the computationally efficient, iterative least-squares algorithm (LSQR) developed by Paige and Saunders (1982).

In PWI, the data vector $\boldsymbol{q}$ is based on the linear constraints on path-averaged S-velocity derived from waveform fitting in the first part of PWI. In fact, the S velocities from the path-averaged models are linearly combined into elements of $\boldsymbol{q}$ in such a way that the elements' uncertainties are uncorrelated [*Nolet,* 1990]. The mixed-determined character of the inverse problem yields its solutions to be non-unique and demands some form of regularization. We regularize the inversion by adding damping equations to $\boldsymbol{Gm} = \boldsymbol{q}$ and solving the resulting system using a least-squares criterion [*Van der Lee and Nolet,* 1997b].

To further deal with the non-uniqueness of solutions to the inverse problem we require the model $\boldsymbol{m}$ to be smooth: $\boldsymbol{m} = \boldsymbol{Sn}$, where S is a smoothing matrix and $\boldsymbol{n}$ a vector of model parameters. For the model derived in this paper S averages $\boldsymbol{m}$ over horizontal regions 600 km in diameter with linearly decreasing weights from the center to the edge of the region. Inserting this model definition in the problem definition $\boldsymbol{Gm} = \boldsymbol{q}$, produces $\boldsymbol{GSn} = \boldsymbol{q}$. We define $\boldsymbol{H} = \boldsymbol{GS}$ and find a damped least-squares solution of $\boldsymbol{Hn} = \boldsymbol{q}$, which gives us the desired smooth model $\boldsymbol{m}$ through $\boldsymbol{m} = \boldsymbol{Sn}$. With this strategy we obtained our preferred, relatively smooth, model NA04 (Plate 2a).

In an alternative scenario we replaced $\boldsymbol{G}$ by a modern version $\boldsymbol{G}'$ that simulates taking off-great-circle sensitivity into account (Figure 2b). $\boldsymbol{G}'$ was computed as $\boldsymbol{G}' = \boldsymbol{GS}$, where $\boldsymbol{G}$ is the sensitivity matrix defined above and S is a matrix that expands the great circle to a more or less elliptical region around it. One row of $\boldsymbol{G}'$ is shown in Figure 2b. We then found a damped least-squares solution of $\boldsymbol{G}'\,\boldsymbol{m} = \boldsymbol{q}$ (Plate 2b).

The different solutions obtained from the great-circle and alternative strategies provide the exact same fit to data vector $\boldsymbol{q}$. Features in the alternative solution (Plate 2b) have larger amplitudes than those in the great-circle solution (Plate 2a) and therefore appear to extend slightly deeper. However, it is unclear which model should be considered a better image of Earth structure. We prefer the model derived with the great-circle theory, because it yields a simpler procedure that can also produce rougher models—like the alternative solution in the Plate 2b—by relaxing the damping and smoothing constraints, whenever appropriate.

Progress in imaging Earth structure more accurately can be made by validating different models (whether solutions to inverse problems or other hypotheses) against different and different types of data sets. Different theories may be used to assess a model's ability to fit these data sets. A joint inversion of multiple data sets will reduce the non-uniqueness of the solution.

4. APPLICATION TO NORTH AMERICA

The waveform data sets of *Frederiksen et al.* [2001] and *Van der Lee* [2002] cover nearly twice the resolved area as

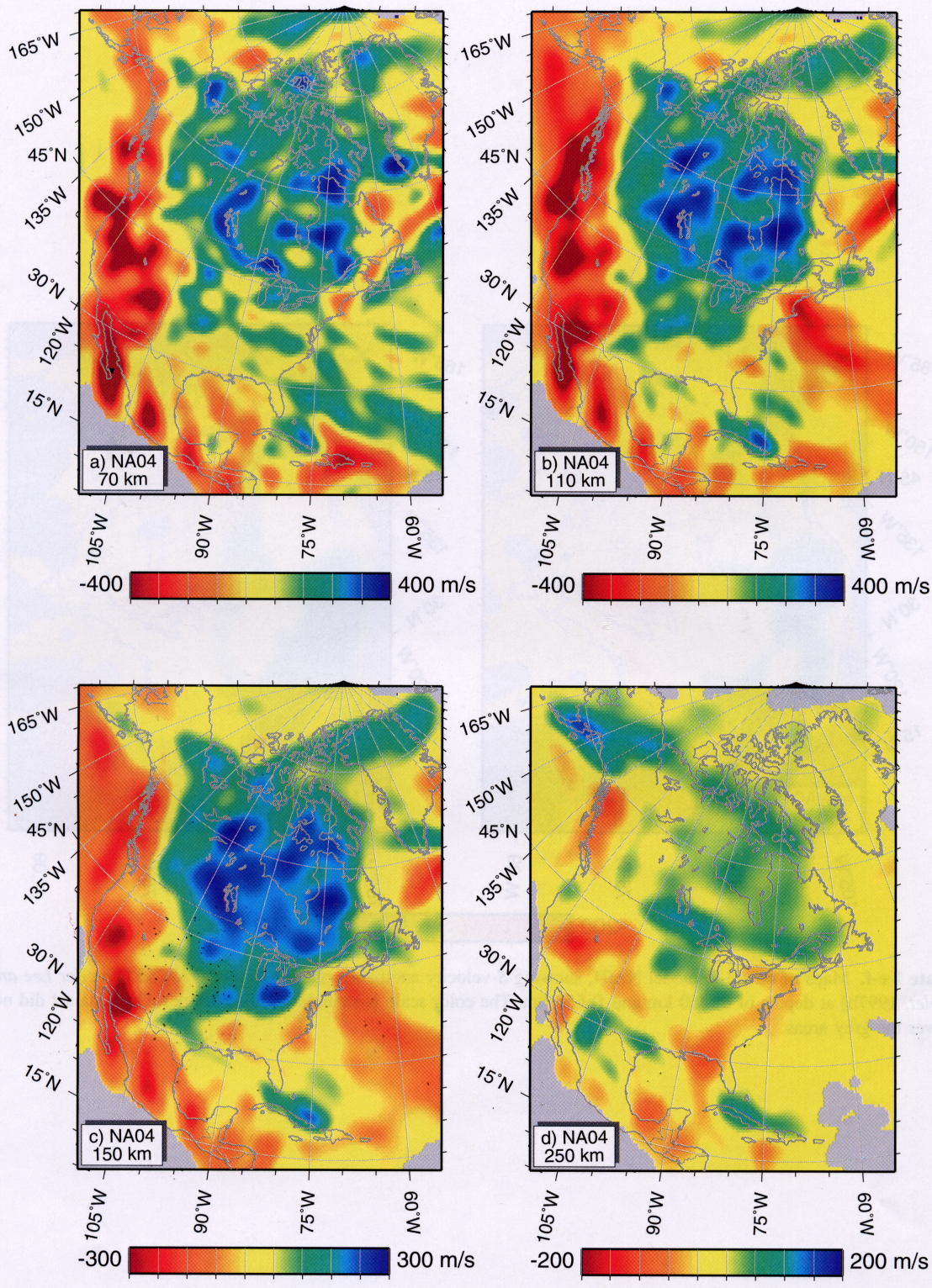

Plate 1 a-d. Maps of new 3-D model NA04, showing *S*-velocity anomalies relative to model MC35 [*Van der Lee and Nolet*, 1997b] at depths of a) 70 km, b) 110 km, c) 150 km, and d) 250 km. The color scale is saturated at its extremes. Our data set did not cover the grey areas.

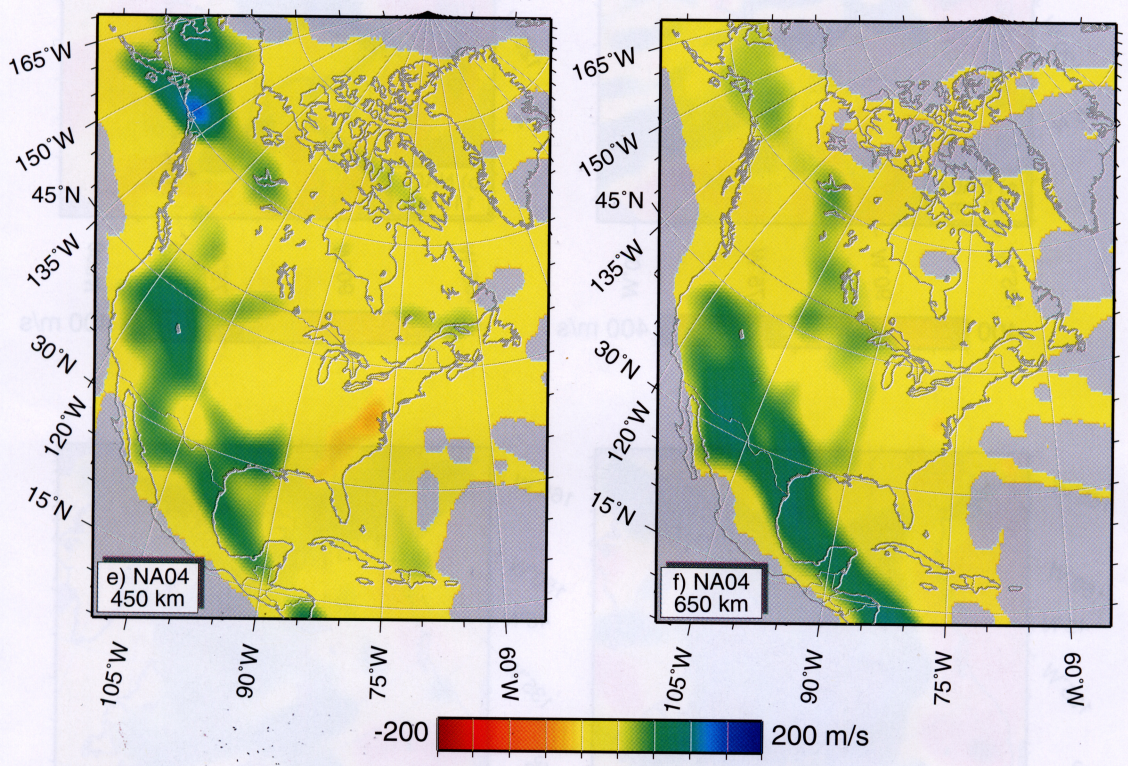

Plate 1 e-f. Maps of new 3-D model NA04, showing *S*-velocity anomalies relative to model MC35 [*Van der Lee and Nolet*, 1997b] at depths of e) 450 km and f) 650 km. The color scale is saturated at its extremes. Our data set did not cover the grey areas.

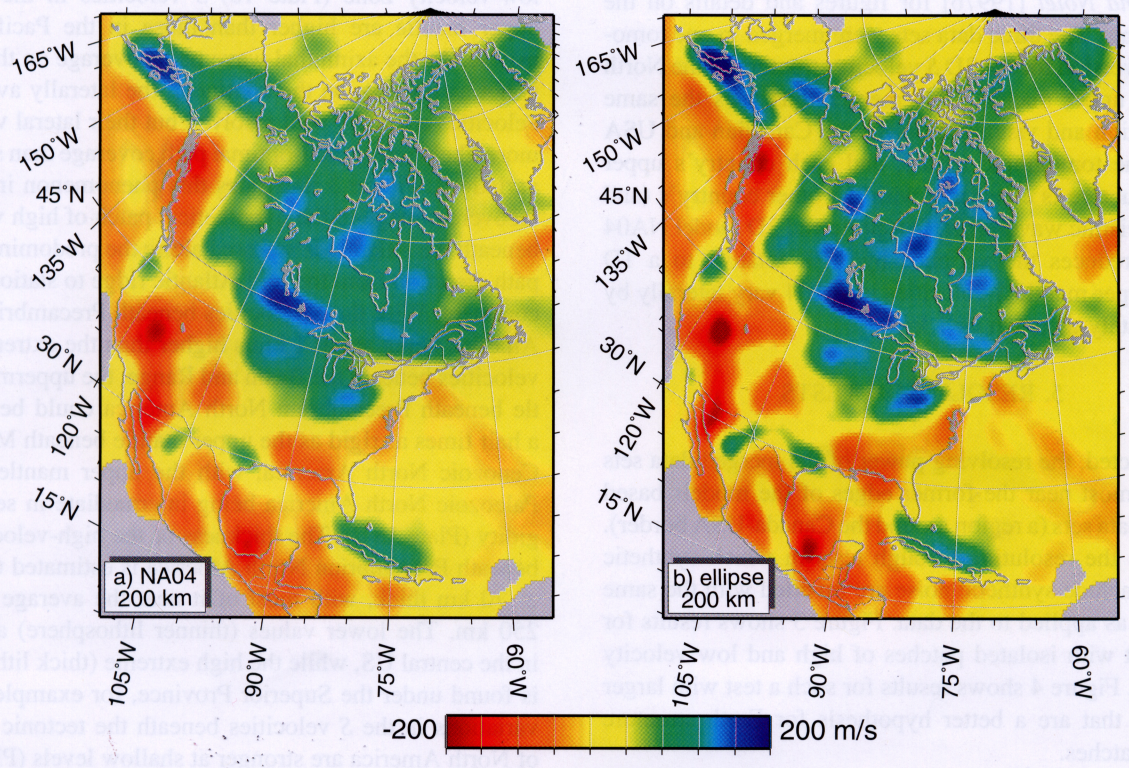

Plate 2. a) Anomalous *S* velocity at a depth of 200 km for NA04. b) Anomalous *S* velocity for a model derived with finite-width sensitivity kernels. The latter model is rougher in that it has larger amplitudes and gradients than NA04. This is a result of transferring the smoothing operation from the velocity model to the sensitivity matrix (see text).

each of the data sets alone. In order to improve the azimuthal coverage for the stations of the stations of the Canadian National Seismic Network [*Baldwin et al.*, 1998] the two data sets were merged and augmented with 160, previously unmodeled, seismograms of Mexican earthquakes recorded by the Canadian stations. Data from other seismic networks were obtained through the IRIS DMC [*Ahern et al.*, 1994]. The three data sets comprise a total of 1379 seismograms, for which the associated great circle wave paths are shown in Figure 1. We refer to *Frederiksen et al.* [2001] and *Van der Lee and Nolet* [1997b] for figures and details on the seismograms. The three data sets were merged in one tomographic inversion for the 3D *S* velocity structure of the North American upper mantle. This merger thus uses the same regularization and visualization for the Canadian and USA parts of the tomograpic model, and each country's upper mantle structure is consistent with the other country's (and its own) seismic waveforms. Our preferred 3D model NA04 (Plate 1) reduces the variance by 97% relative to a 1D model. Upper mantle *S* velocities in NA04 vary laterally by approximately as much as 1 km/s.

5. RESOLUTION TESTS

As expected, the resolving power of the merged data sets improves most near the former edges of the models based on single data sets (a region around the Canada-USA border). We assess the resolution through tests in which synthetic data that include synthetic noise are inverted with the same procedure as applied to the data. Figure 3 shows results for such a test with isolated patches of high and low velocity anomalies. Figure 4 shows results for such a test with larger anomalies that are a better hypothesis for Earth structure than the patches.

The tests show that our data set can resolve the magnitude and shape of anomalies on the scale of tectonic domains our data set where station coverage is densest, which is one of the motivations behind the USArray project. Elsewhere and for smaller-scale anomalies the magnitudes are underestimated. Figures 3 and 4 also illustrate how sharp transitions and sudden bends in the shapes of anomalies are smoothed out, and that smearing of anomalies is rare beneath the continent.

Another positive effect of high station density (such as that of USArray) is its ability to accurately image the magnitude of velocity anomalies over an extensive depth range. Including seismograms from the dense MOMA array [*Fischer et al.*, 1996] results in a smaller decrease in resolving power with depth than usual in surface-wave tomography, which in turn results in more accurate estimates of lithospheric thickness and sub-lithospheric low velocities [*Van der Lee*, 2002].

6. PREFERRED MODEL

Our new model NA04 does not differ significantly from its predecessors [*Frederiksen et al.*, 2001; *Van der Lee and Nolet*, 1997b] in terms of the main structural features of the North American upper mantle. We summarize these features here. At both the levels of the lithosphere (Plate 1a) and the low-velocity zone (Plate 1b) *S* velocities in the Atlantic upper mantle are higher than those in the Pacific upper mantle. As the azimuthal wave path coverage on the oceans is not as good as on the continent, the laterally averaged *S* velocities are fairly well resolved but their lateral variations more likely reflect non-optimal path coverage than structural variations. Figure 3 illustrates this phenomenon in that the recovered image of the hypothetical patch of high velocities beneath the Atlantic is smeared along the predominant wave path direction from the mid-Atlantic ridge to stations on the continent. With the *S* velocities beneath Precambrian North America being about 1 km/s higher than the extremely low velocities beneath the Basin and Range, the uppermost mantle beneath Precambrian North America could be one and a half times as rigid as the upper mantle beneath Meso- and Cenozoic North America, with the upper mantle beneath Paleozoic North America being intermediate in seismic rigidity (Plate 1a-d). The thickness of the high-velocity layer beneath Precambrian North America is estimated to be 250 $\pm$ 70 km thick, with most of it near the average value of 250 km. The lower values (thinner lithosphere) are found in the central US, while the high extreme (thick lithosphere) is found under the Superior Province, for example. Lateral variations in the *S* velocities beneath the tectonic domains of North America are stronger at shallow levels (Plate 1a-c) and could be due in part to unmodeled fine-scale structure of the crust. On the other hand, resolution tests have shown that some lateral velocity variations within tectonic domains can be resolved with our data. We believe that the upper-mantle velocity within tectonic domains indeed varies laterally but feel that for a detailed interpretation fine crustal structure needs to be better accounted for. High velocity anomalies at the bottom of the upper mantle (Plate 1c,d) align with lower mantle images of the subducted Farallon [*Grand*, 1994] and Kula plates [*Bunge and Grand*, 2000]. NA04 indicates that trailing fragments of these subducted oceanic plates still reside in the transition zone, implying a slower descent than in geodynamic models [*Lithgow-Bertelloni and Richards*, 1997; *Bunge and Grand*, 2000]. NA04 shows high upper-mantle velocities associated with subduction of the Pacific plate beneath the Aleutian arc (Plate 1).

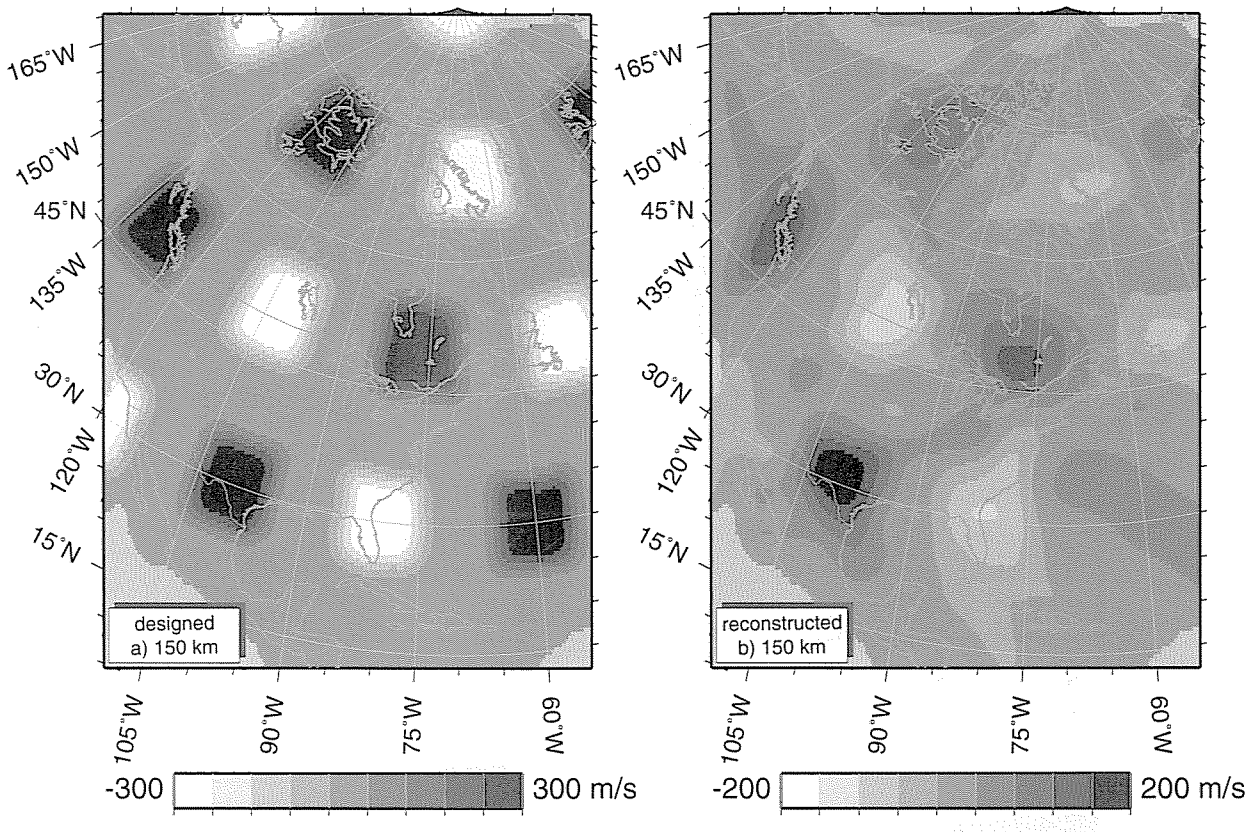

Figure 3. a) *S* velocity anomalies designed as arbitrarily distributed fast and slow spheres. b) *S* velocity anomalies reconstructed with available data coverage.

NA04 confirms and better resolves the absence of geologically expected high-velocities in the upper mantle beneath the Wyoming craton (Plate 1a-d). A V-shaped dent below 150 km in the high-velocity cratonic lithosphere beneath New England, first identified in NA95 [*Van der lee and Nolet*, 1007b], is also confirmed by NA04, as well as by more regional studies [*Li et al.*, 2002; *Menke and Levin*, 2002]. The cratonic, high-velocity lithosphere beneath Precambrian North America is sharply confined to southwest of Baffin Bay, west of the Appalachians, north of the Ouachitas, east of the Rocky Mountains, and south of the Arctic Ocean. The cratonic lithosphere beneath the Canadian shield has higher *S* velocities than that beneath Precambrian basement that is covered with Phanerozoic sediments. The lowest *S* velocities of NA04 are concentrated beneath the Gulf of California, northern Mexico, and the Basin and Range Province. Except for those beneath the Basin and Range, these low velocities do not extend below 200 km and can be explained with reasonably high uppermost mantle temperatures [*Goes and Van der Lee*, 2002]. The low velocities beneath the Basin and Range extend to 300 km, and their location coincides with that of the earliest onset of slab window formation [*Dickinson*, 1997]. The North American craton seems to be disconnected from the lithosphere of Greenland. While our resolving power below Greenland is reduced, anomalies beneath Baffin Bay can be resolved by our data set.

7. CONCLUSIONS

The dense station spacing of USArray will likely increase the resolving power in surface wave tomography significantly. We further note that USArray-type station spacings and array size are necessary for an accurate separation of the scattered wavefield from the direct wavefield. Scientific collaborations at the national level at which USArray operates will reduce the non-uniqueness of tomographic models by requiring them to fit multiple data sets and/or independent hypotheses about North-American upper mantle structure.

The application of the surface-wave tomographic method PWI to our merged independent waveform data sets has produced a new 3D *S* velocity model for the North American upper mantle. We used the new model to compare the upper-mantle *S* velocity beneath the northwest Atlantic with that

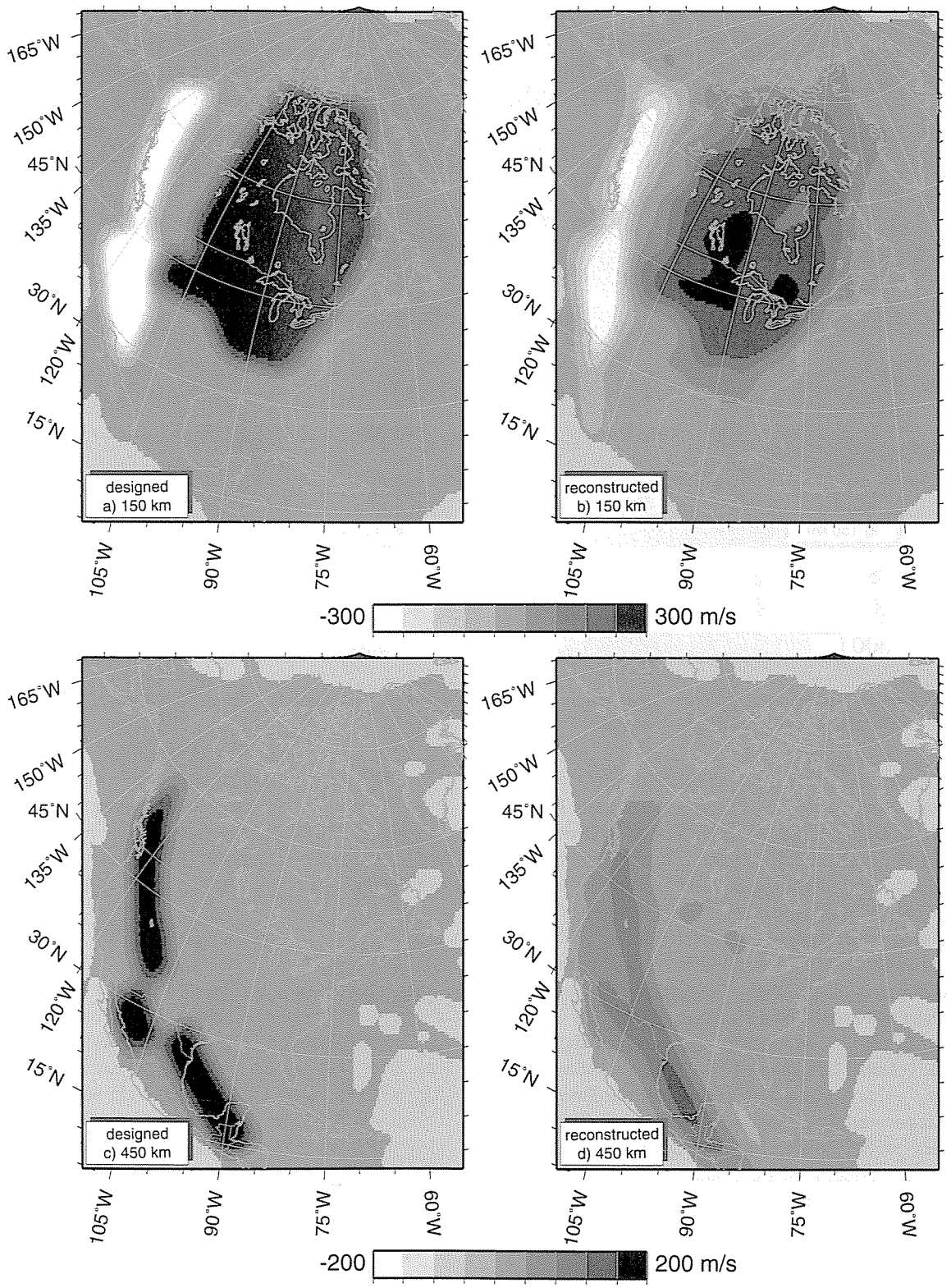

Figure 4. a) *S* velocity anomalies designed as simple, geologically motivated, structural features at a depth of 150 km, and c) 450 km. b) *S* velocity anomalies reconstructed with available data coverage at 150 km, and d) 450 km.

of the northeast Pacific. Within the continent, we examined the rigidity and depth extent of the high-velocity Precambrian lithosphere and of the low velocities beneath western North America, as well as the lateral extent of and variations in these. Subducted trailing fragments of both the Farallon and Kula plates are found in the transition zone. Geodynamic implications of our findings are the subject of ongoing study. This paper's purpose was to discuss and demonstrate a surface wave tomography technique in the context of USArray imaging potential.

Acknowledgments. This work was supported by NSF grant EAR-0346200. We thank Alan Levander and Guust Nolet, for admirable patience and Karen Fischer for a helpful review.

REFERENCES

Burnham, C. W., Importance of volatile constituents, *in Evolution of Igneous Rocks,* edited by H. D. Yoder, pp. 439-482, Princeton University Press, Princeton, N. J., 1979.

Cowan, J. M.., Elasticity of Mantle Phases at High Temperature, *J. of Geophys. Res.,* 95, 439-482, 1999.

Ahern, T., and Members of the FDSN, Federation of Digital Seismograph Networks Station Book, *Inc. Res. Inst. for Seismol.*, Seattle, Wash., 1994.

Aki, K., A. Christofferson, and E.S. Husebye, Determination of the three-dimensional seismic structure of the lithosphere, *Geophys. J. Astr. Soc.*, 82, 277-296, 1977.

Baldwin, R.E., K.I. Beverley, and G.C. Rogers, The Canadian National Seismic Network in Western Canada, *Seism. Res. Lett.*, 69, 155, 1998.

Boschi, L., and G. Ekström, New images of the Earth's upper mantle from measurements of surface wave phase velocity anomalies, *J. Geophys. Res.*, 107, doi:10.1029/2000JB000059, 2002.

Boschi, L., G. Ekström, and B. Kustowski, Multiple resolution surface wave tomography: the Mediterranean basin, *Geophys. J. Int.*, 157, 293-304, 2004.

Bowring, S.A., and I.S. Williams, Priscoan (4.00-4.03 Ga) orthogneisses from northwestern Canada, *Contrib. Mineral. Petrol.*, 134, 3-16, 1999.

Bunge, H.P., and S.P. Grand, Mesozoic plate-motion history below the northeast Pacific Ocean from seismic images of the subducted Farallon slab, *Nature*, 405, 337-340, 2000.

Chulick, G.S., and W.D. Mooney, Seismic Structure of the Crust and Uppermost Mantle of North America and Adjacent Oceanic Basins: A Synthesis, *Bull. Seism. Soc. Am.*, 92, 2090-2109, 2002.

Cara, M., Lateral variations of *S* velocity in the upper mantle from higher Rayleigh modes, *Geophys. J. R. Astron. Soc.*, 57, 649-670, 1979.

Dickinson, W.R. Tectonic implications of Cenozoic volcanism in coastal California, *Geol. Soc. Am. Bull.*, 109, 936-954, 1997.

Dziewonski, A.M., A.L. Hales, and E.R. Lapwood, Parametrically simple Earth models consistent with geophysical data, *Phys. Earth Planet. Inter.*, 10, 12-48, 1975.

Dziewonski, A.M., B.H. Hager, and R.J. O'Connell, Large-scale heterogeneities in the lower mantle, *J. Geophys. Res.*, 82, 239-255, 1977. Dziewonski, A.M., G.

Ekström, and M.P. Salganik, Centroid-moment tensor solutions for July-September 1991, *Phys.Earth Planet. Inter.*, 72, 1-11, 1992.

Engebretson, D.C., A. Cox, and A.G. Gordon, Relative Motions Between Oceanic and Continental Plates in the Pacific Basin, *Geol. Soc. Am. special paper*, 206, 59 pp, 1985.

Ekström, G. and A.M. Dziewonski, The unique anisotropy of the Pacific upper mantle, *Nature*, 394, 168-172, 1998.

Fischer, K.M., M.E. Wysession, T.J. Clarke, M.J. Fouch, G.I. Al-Eqabi, P.J. Shore, R.W. Valenzuela, A. Li, and J.M. Zaslow, *The 1995-1996 Missouri to Massachusetts Broadband seismometer deployment*, IRIS Newsletter, 15, p 6-9, 1996.

Frederiksen, A.W., M.G. Bostock, and J.F. Cassidy, *S* wave velocity structure of the Canadian upper mantle, *Phys. Earth Planet. Inter.*, 124, 175-191, 2001.

Friederich, W., The *S*-velocity structure of the East Asian mantle from inversion of shear and surface waveforms, *Geophys. J. Int.*, 153, 88-102, 2003.

Gee, L.S., and T.H. Jordan, Generalized seismological data functionals, *Geophys. J. Int.* 111, 363-390, 1992.

Goes, S., and S. van der Lee, Thermal structure of the North American uppermost mantle inferred from seismic tomography, *J. Geophys. Res.*, 107, DOI:10.1029/2000JB000049, 2002.

Grand, S.P., Mantle shear structure beneath the Americas and surrounding oceans, *J. Geophys. Res.*, 99, 11,591-11,621, 1994.

Herrin, E., and T. Goforth, Phase-matched filters: Application to the study of Rayleigh waves, *Bull. Seism. Soc. Am.*, 67, 1259-1275, 1977.

Hoffman, P. F., United plates of America, the birth of a craton: Early Proterozoic assembly and growth of Laurentia, *Annu. Rev. Earth Planet. Sci.*, 16, 535-603, 1988.

Jeffreys, H. and K.E. Bullen, Seismological Tables, *British Association Seismological Committee*, London, 1940.

Kennett, B.L.N., E.R. Engdahl and R. Buland, Constraints on seismic velocities in the Earth from traveltimes, *Geophys. J. Int.*, 122, 108-124, 1995.

Li, X., and B. Romanowicz, Global mantle shear velocity model developed using nonlinear asymptotic coupling theory, *J. Geophys. Res.*, 101, 22245-22272, 1996.

Li, A., D.W. Forsyth, and K.M. Fischer, Shear velocity structure and azimuthal anisotropy beneath eastern North America from Rayleigh wave inversion, *J. Geophys. Res.*, 108, DOI:10.1029/2002JB002259, 2002.

Lithgow-Bertelloni, C., and M.A. Richards, The dynamics of Cenozoic and Mesozoic plate motions, *Reviews of Geophysics*, 27, 32-72, 1998.

Lebedev, S. and G. Nolet, Upper mantle beneath Southeast Asia from *S* velocity tomography, *J. Geophys. Res.*, 108, DOI:10.1029/2000JB000073, 2003.

Levshin, A.L., Effects of lateral inhomogeneities on surface wave amplitude measurements, *Ann. Geophys.*, 3, 511-518, 1985.

Marone, F., S. van der Lee, D. Giardini, 3-D upper mantle *S*-velocity model for the Eurasia-Africa plate boundary region, *Geophys. J. Int.*, 158, 109-130, 2004.

Marquering, H., and R. Snieder, Surface-wave mode coupling for efficient forward modelling andinversion of body-wave phases, *Geophys. J. Int.*, 120, 186-208, 1995.

Marquering, H., G. Nolet, and F.A. Dahlen, Three-dimensional waveform sensitivity kernels, *Geophys. J. Int.*, 132, 521-534, 1998.

Meier, T., S. Lebedev, G. Nolet, and F.A. Dahlen, Diffraction tomography using multimode surface waves, *J. Geophys. Res.*, 102, 8255-8267, 1997.

Menke, W., and V. Levin, Anomalous seaward dip of the lithosphere-asthenosphere boundary beneath northweastern USA detected using differential-array measruments of Rayleigh waves, *Geophys. J. Int.*, 149, 413-421, 2002.

Nishimura, C.E. and W.F. Forsyth, The anisotropic structure of the upper mantle in the Pacific, *Geophys. J.*, 96, 203-229, 1989.

Nolet, G., Partitioned waveform inversion and two-dimensional structure under the network of autonomously recording seismographs, *J. Geophys. Res.*, 95, 8499-8512, 1990.

Nolet, G., Solving large linearized tomographic problems, in "*Seismic tomography: Theory and practice*", eds. H.M. Iyer and K. Hirahara, Chapman & Hall, London, 1993.

Paige, C.C., and M.A. Saunders, ALGORITHM 583 LSQR: sparse linear equations and least squares problems, *ACM TOMS*, 8, 195-209, 1982.

Pilidou, S., K. Priestley, O. Gudmundsson, and E. Debayle, Upper mantle *S*-wave speed heterogeneity beneath the North Atlantic and the surrounding region from regional surface wave tomography, *Geophys. J. Int.*, 159, 1057-1076, 2004.

Ritzwoller, M.H., N.M. Shapiro, M.P. Barmin, and A.L. Levshin, Global surface wave diffraction tomography, *J. Geophys. Res.*, 107, DOI:10.1029/2002JB001777, 2002.

Snieder, R., Large-scale waveform inversions of surface waves for lateral heterogeneity; 1, Theory and numerical examples, *J. Geophys. Res.*, 93, 12055-12065, 1988.

Spetzler, J., J. Trampert, and R. Snieder, The effect of scattering in surface wave tomography, *Geophys. J. Int.*, 149, 755-767, 2002.

Stern, R.S., and W. Bleeker, Age of the world's oldest rocks refined using Canada's SHRIMP: the Acasta Gneiss Complex, Northwest Territories, Canada, *Geoscience Canada*, 25, 27-33, 1998.

Stock, J., and P. Molnar, Uncertainties and implications of the Late Cretaceous and Tertiary position of North America relative to the Farallon, Kula and Pacific plates, *Tectonics*, 7, 1339-1384, 1988.

Tromp, J., and F.A. Dahlen, Variational principles for surface wave propagation on a laterally heterogeneous Earth, II, Frequency-domain JWKB theory, *Geophys. J. Int.*, 109, 599-619, 1992.

Van der Lee, S. and G. Nolet, Seismic image of the subducted trailing fragments of the Farallon plate, *Nature*, 386, 266-269, 1997a.

Van der Lee, S. and G. Nolet, Upper-mantle *S*-velocity structure of North America, *J. Geophys. Res.*, 102, 22,815-22,838, 1997b.

Van der Lee, S. Observations and origin of Rayleigh wave amplitude anomalies, *Geophys. J. Int.*, 135, 691-199, 1998.

Van der Lee, S. Deep below North America, *Science*, 294, 1297-1298, 2001.

Van der Lee, S., High-resolution estimates of lithospheric thickness from Missouri to Massachusetts, USA, *Earth Planet. Sc. Lett.*, 203, 15-23, 2002.

Woodward, R.L., and G. Masters, Lower-mantle structure from ScS-S differential travel times, *Nature*, 352, 231-233, 1991.

Wu, F.T., A.L. Levshin, V.M. Kozhevnikov, Rayleigh wave group velocity tomography of Siberia, China and the vicinity, *Pure and Applied Geophysics*, 149, 447-473, 1997.

Xu, Y. and D.A. Wiens, Upper mantle structure of the southwest Pacific from regional waveform inversion, *J. Geophys. Res.*, 102, 27439-27451, 1997.

Yoshizawa, K. and B.L.N. Kennett, Determination of the influence zone for surface wave paths, *Geophys. J. Int.*, 149, 440-453, 2002.

Zhao, L. and T.H. Jordan, Sensitivity of frequency-dependent traveltimes to laterally heterogeneous, anisotropic Earth structure, *Geophys. J. Int.*, 133, 683-704, 1998.

Zhou, Y., F.A. Dahlen, and G. Nolet, Three-dimensional sensitivity kernels for surface wave observables, *Geophys. J. Int.*, 158, 142-168, 2004.

Zielhuis, A., and G. Nolet, Shear-wave velocity variations in the upper mantle beneath central Europe, *Geophys. J. Int.*, 117, 695-715, 1994.

Suzan van der Lee, Department of Geological Sciences, Northwestern University, 1850 Campus Drive, Evanston IL 60201, USA.

Andrew Frederiksen, Department of Geological Sciences, University of Manitoba, Winnipeg R3T 2N2, Canada.